Sample-profile estimate for fast atomic force microscopy

Srinivasa Salapaka[a)]
Department of Mechanical and Industrial Engineering, University of Illinois at Urbana-Champaign, Urbana, Illinois 61801

Tathagata De[b)]
Department of Electrical and Computer Engineering, Iowa State University, Ames, Iowa 50011

Abu Sebastian[c)]
IBM Zurich Research Laboratory, 8803 Rueschlikon, Switzerland

(Received 28 January 2005; accepted 27 June 2005; published online 29 July 2005)

In this letter, a design scheme that achieves an optimal tip-sample force regulation with an ideal topography image reconstruction is presented. It addresses the problem of obtaining accurate sample profiles when scanning at high bandwidth while maintaining a constant cantilever-tip sample force in atomic force microscopes. In this design scheme, the objective of maintaining a constant tip-sample force while scanning at high bandwidth does not impose limitations on the reconstruction of the sample topography. It is shown that the proposed scheme provides a faithful replica of the sample at all relevant scanning speeds limited only by the inaccuracy in the model for the atomic force microscope. This provides an improvement over existing designs where the sample profile reconstruction is typically bandwidth limited. Comparison with the existing methods of using the control signal as the image is provided. The experimental results corroborate the theoretical development. © *2005 American Institute of Physics*. [DOI: 10.1063/1.2006213]

The model of the atomic force microscope (AFM) in contact-mode operation is described in Figs. 1 and 2, where in the latter, device components are represented by *transfer functions*. They represent linear dynamics of components about a nominal operating point. In Fig. 2, G_z is the transfer function that gives the dynamical relation between the vertical positioner position and the voltage input to the positioner. In this model (similar models are studied in Refs. 1 and 2), the surface topography appears as a "disturbance" signal d, which tries to deviate the cantilever deflection signal y, from its set-point deflection; the regulation objective is to reject the disturbance to maintain a constant deflection signal. If we assume that the cantilever transfer function G_c is a constant, which is a good approximation because microcantilevers have much larger bandwidths than the vertical positioners, then $\tilde{d}$ represents the scaled sample profile.

In typical contact-mode operation, the control signal u is used to obtain an estimate of the sample topography $\tilde{d}$. The rationale for using the control signal u as a profile estimate signal is explained by analyzing the feedback loop shown in Fig. 2. A good set-point regulation over a prespecified bandwidth is achieved by designing $K(j\omega)$ to have high gains over the bandwidth. This is seen from the transfer function from r to e given by $1/[1+G(j\omega)K(j\omega)]$, which is small when $K(j\omega)$ is large. Moreover the transfer function from the sample profile $\tilde{d}$ to the control signal u is $K(j\omega)/[1+K(j\omega)G(j\omega)]$. This expression can be approximated by $1/G(j\omega)$ for large $K(j\omega)$. Low-bandwidth imaging do not excite the high-frequency dynamics of the positioner. Therefore the transfer function $G(j\omega)$ can be assumed to be a constant and the control signal u is then a good estimate of the sample topography.

However, for high-bandwidth operation, the dynamics of the positioner has to be addressed. To achieve good regulation the control will compensate for the positioner dynamics and thus the control signal will no longer be an accurate estimate of the sample profile. Accordingly an important question to be addressed is whether the positioner dynamics $G(j\omega)$ imposes any fundamental limitation on the imaging aspects in scanning probe microscopes. More precisely, if the controllers are designed to *reject* the topography signal $\tilde{d}$ (as imposed by regulating the deflection signal), then the limitations imposed on the *reconstruction* of the topography have to be determined. The discussion above and in the earlier literature[1–4] indicate that a compromise has to be struck between reconstructing the topography image and the imaging bandwidth. One of the fundamental contributions of this letter is that the regulation objective of maintaining a given set point does not conflict with the image reconstruction objective. This result is not intuitive given the fact that the positioner dynamics cannot be inverted.

Recent related research efforts that are aimed at obtaining images at high-bandwidth operation include methods that operate away from the resonant frequencies of the vertical positioner,[3] use better sample-profile estimate signals instead

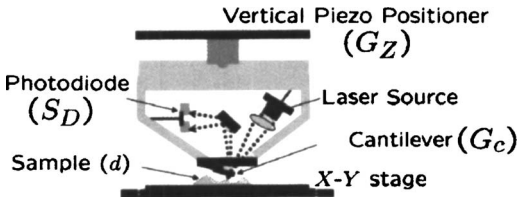

FIG. 1. A schematic of an atomic force microscope. The cantilever is attached to a vertical positioner. The cantilever deflection is sensed, and a feedback controller moves the positioner to maintain a constant deflection.

[a)]Electronic mail: salapaka@uiuc.edu
[b)]Electronic mail: tatha@iastate.edu
[c)]Electronic mail: ase@zurich.ibm.com

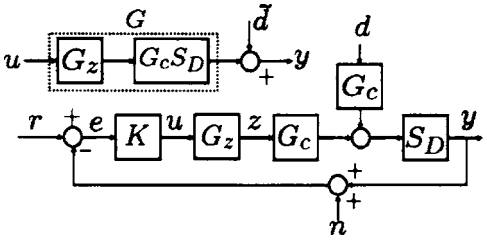

FIG. 2. The block diagram model of the AFM, where G_c, G_z, K, S_D model the cantilever, piezoelectric positioner, controller, and the deflection transducer, respectively. y and n are the cantilever deflection and transducer noise, respectively. d models the sample topography. G represents a combination of positioner, cantilever, and transducer dynamics. The cantilever has a high resonant frequency and is assumed to be a constant over the frequency region of interest. Hence $\tilde{d}$ is a scaled version of the sample topography.

of the control signal,[1] and simulate positioner dynamics to obtain better estimates of the sample profile.[2] However, these methods suffer from limited imaging bandwidths. The main distinguishing feature of the design proposed in this letter compared with existing methods is that it produces an image signal that provides an accurate image *independently* of the bandwidth achieved by the feedback law and the dynamics of the positioner.

We employ an optimal control ($\mathcal{H}_\infty$) (Ref. 5) design scheme from systems theory to achieve the multiple objectives of set-point regulation (captured by the sensitivity transfer function $S(j\omega)=1/[1+G(j\omega)K(j\omega)]$, which relates the set-point r to the deflection error e), immunity from high-frequency sensor noise (captured by $T(j\omega)=[G(j\omega)K(j\omega)]/[1+G(j\omega)K(j\omega)]$, the transfer function from noise n to e), and bound on the control effort for positioner actuation (captured by KS, the transfer function from r to u). This scheme yields a controller that minimizes the peak magnitude in the frequency response of $(W_S S)^2+(W_T T)^2+(W_u KS)^2$, where W_S, W_T, and W_u are the frequency-dependent weights on the objectives. The main steps in this scheme are (1) choosing appropriate weights W_S, W_T, and W_u, and (2) forming a generalized positioner transfer function from $[\tilde{d}\ u]$ to $[z_1\ z_2\ z_3\ e]$ (see Fig. 3) given by P and (3) solving the associated optimal control problem using software (e.g., HINFSYN in Matlab) that yields the controller K. Detailed exposition of this method and its advantages to scanning probe applications are provided in Refs. 4 and 6. Note that in these works, the objectives addressed do not include that of sample topography reconstruction. Thus at this design stage, the tip-sample force regulation (set-point regulation) objective is not compromised because of the objective of the sample topography reconstruction. It is demonstrated now that this scheme also yields the optimal sample topography reconstruction signal $\hat{d}$.

The proposed estimate signal $\hat{d}$ of the sample profile $\tilde{d}$ is obtained by exploiting the structure of the controller K that results from the optimal control design for set-point regulation. The optimal controller has a model of the vertical positioner in it that is used to account for the latter's dynamics in estimating $\tilde{d}$. It has a *quasiobserver* structure, i.e., the differential equations that describe the controller have similar structure to the differential equations that describe the generalized positioner system P. Indeed with the P dynamics described by

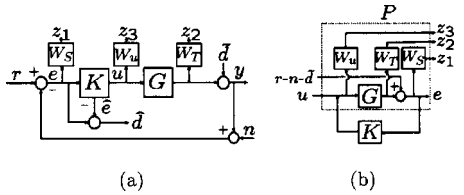

FIG. 3. (a) W_S, W_T, and W_u are the weights used for designing the optimal controller K. $\hat{e}$ is a function of controller states. $\hat{d}=\hat{e}-e$ is the proposed signal to estimate the sample profile. (b) The block diagram in (a) can be redrawn as shown in (b). P is the generalized positioner transfer function which is used in the optimal control scheme.

$$\dot{x} = Ax + B_1\tilde{d} + B_2 u,$$

$$e = C_2 x - \tilde{d},$$

the optimal controller synthesis[5] yields a controller K whose dynamics is of the form

$$\dot{\hat{x}} = A\hat{x} + B_1\hat{w} + B_2 u + Z_\infty L_{2\infty}(\hat{e} - e),$$

$$\hat{e} = C_2\hat{x},$$

$$u = F_{2\infty}\hat{x},$$

where $\hat{x}$ is an estimate of the states of P, and the vector $\hat{w}$ is a function of $\hat{x}$. Here the matrices Z_∞, $F_{2\infty}$, and $L_{2\infty}$ are as described in (Refs. 5, pp. 451–452). Note that the estimate of the error signal $\hat{e}$ does not contain $\tilde{d}$, whereas the error signal e contains the sample profile $\tilde{d}$. This difference is exploited by defining the estimate $\hat{d}$ of the sample profile $\tilde{d}$ by $\hat{d}\triangleq\hat{e}-e$; i.e., $\hat{d}=C_2\hat{x}-e$ [see Fig. 3(a)]. Thus, the optimal set-point controller synthesis needs to be augmented by the step of forming $\hat{e}$-e to provide an estimate of $\tilde{d}$. Remarkably it can be shown from the above equations that the transfer function $T_{\tilde{d}\hat{d}}$ between the estimated sample profile $\hat{d}$ and the sample profile $\tilde{d}$ is identically equal to one, independent of the scanning frequency; i.e., $T_{\tilde{d}\hat{d}}(j\omega)=1$ for all frequencies ω. This implies that $\hat{d}$ yields an accurate image, independent of frequency content in the sample topography. This is in contrast to the control signal, which gives a good estimate only if the topography signal $\tilde{d}(t)$ has frequency content within the bandwidth achieved by the controller. There are other controller architectures for which a similar result holds (i.e., $T_{\tilde{d}\hat{d}}(j\omega)=1$ for all ω). A detailed exposition of such architectures and associated proofs have been submitted to the *International Journal of Robust and Nonlinear Control*.[7] Thus this letter focuses on one architecture where the tip-sample force regulation objective does not conflict with the image reconstruction objective.

Experiments were performed to test the theoretical results. A gold calibration grid with squares of 180 nm height every 10 μm was used for imaging using the $\hat{d}$ signal. This experiment was done using a molecular force probe (MFP-3D) system from Asylum Research Inc., Santa Barbara, CA. This image was compared with the one obtained from the control signal u. Figure 4(a) shows the experiment in which the grating was scanned at 10 Hz. The corresponding control signal u and the proposed estimate signal $\hat{d}$ were recorded. It is observed that both the control signal and the proposed

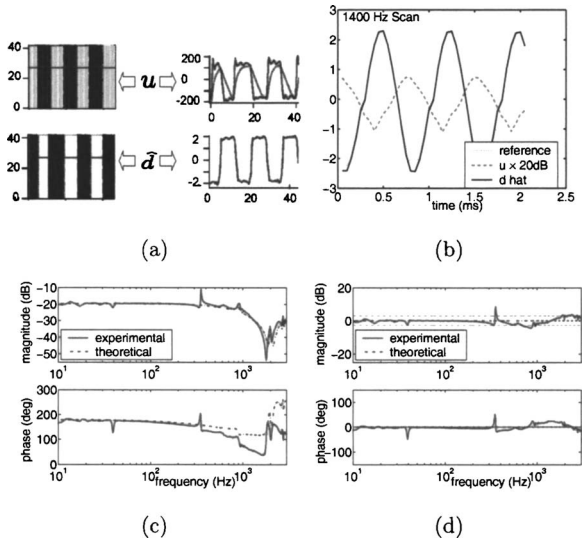

FIG. 4. (a) Experimental data shows that significantly superior images are obtained by using the proposed imaging signal $\hat{d}$ compared with using the control effort u as the sample topography estimate. (b) Experimental data shows that the proposed signal $\hat{d}$ gives an accurate image of 1400 Hz sine wave topography. The control signal, u becomes attenuated and incurs significant phase lag from the sample profile. (c) The experimental frequency response of the control effort u to sample topography. (d) The experimental frequency response of the estimate $\hat{d}$ to sample topography.

signal provide good images of the calibration sample. Even at these low frequencies, the image with the proposed signal is better than the image with the u signal, which shows spurious oscillations. The differences in images from $\hat{d}$ and u were more significant in a faster scan done at 1400 Hz [see Fig. 4(b)]. Owing to limitations on the lateral scanning capability of the device, it was not possible to generate a 1400 -Hz topography signal using the calibration grid and hence, in this experiment, a sinusoidal signal at 1400 Hz was generated in the DSP and was added to the real-time deflection data. The experimental results show that the proposed signal $\hat{d}$ tracks the reference signal near perfectly even at these high bandwidths, whereas the control signal u, fails to do so. The transfer functions from the $\tilde{d}$ signal to the $\hat{d}$ and u signals ($T_{\tilde{d}\hat{d}}$ and $T_{\tilde{d}u}$, respectively) were obtained experimentally over a bandwidth of 3000 Hz. Figure 4(c) shows that the bandwidth of the transfer function $T_{\tilde{d}u}$ is approximately 800 Hz, whereas the magnitude of $T_{\tilde{d}\hat{d}}$ [in Fig. 4(d)] is within 3 dB for the entire range (up to 3000 Hz) considered. The phase plots reveal a considerable phase drop for $T_{\tilde{d}u}$, and near zero phase for $T^{\tilde{d}\hat{d}}$. This explains the difference found in the trace and retrace scans when using the u signal for the image. These experiments corroborate the theoretically obtained result that $T_{\tilde{d}\hat{d}}=1$ for all ω. As the optimal controller has a model of AFM system P embedded in it, any inaccuracy in the modeling of the AFM has a detrimental effect on the sample topography reconstruction. However, experiments show that these effects are small and the ongoing analysis shows that there exists a tuning parameter that enables a trade off between robustness of image reconstruction and scanning bandwidth.

S.S. acknowledges the financial support of NSF Grant No. ECS 0449310 CAR. T.D. acknowledges the support of NSF Grants No. CMS 0301516 and CMS 0201560.

[1] A. Sebastian, J. P. Cleveland, and M. V. Salapaka, Proceedings of the IEEE Conference on Decision and Control, Hawaii, 2003 (IEEE, New York, 2003), pp. 3443–3444.
[2] G. Schitter, F. Allgower, and A. Stemmer, Rev. Sci. Instrum. **15**, 108 (2004).
[3] K. Rifai, O. Rifai, and K. Youcef-Toumi, Proceedings of the American Control Conference, Boston, MA, 2004, pp. 3128–3133.
[4] G. Schitter, P. Menold, H. F. Knapp, F. Allgower, and A. Stemmer, Rev. Sci. Instrum. **72**, 3320 (2001).
[5] K. Zhou, J. Doyle, and K. Glover, *Robust and Optimal Control* (Prentice Hall, Upper Saddle River, NJ, 1996).
[6] S. Salapaka, A. Sebastian, J. P. Cleveland, and M. V. Salapaka, Rev. Sci. Instrum. **73**, 3232 (2002).
[7] S. Salapaka, D. Tathagata, and A. Sebastian, Int. J. Robust Nonlinear Control (to be published).